

## New Misfit Cobaltites $[\text{Pb}_{0.7}\text{A}_{0.4}\text{Sr}_{1.9}\text{O}_3][\text{CoO}_2]_{1.8}$ ( $\text{A} = \text{Hg, Co}$ ) with Large Thermopower

D. Pelloquin, A. Maignan,\* S. Hébert, C. Martin, M. Hervieu, C. Michel, L. B. Wang, and B. Raveau

Laboratoire CRISMAT, UMR CNRS ISMRA 6508, 6 bd Maréchal Juin, 14050 CAEN Cedex, France

Received January 23, 2002. Revised Manuscript Received April 18, 2002

New misfit cobaltites, containing lead and mercury, have been synthesized,  $[\text{Pb}_{0.7}\text{Sr}_{1.9}\text{Co}_{0.4}\text{O}_3][\text{CoO}_2]_{1.8}$  and  $[\text{Pb}_{0.7}\text{Hg}_{0.2}\text{Sr}_{1.9}\text{Co}_{0.2}\text{O}_3][\text{CoO}_2]_{1.8}$ . Their structural study, using high resolution electron microscopy and X-ray powder diffraction, shows that the samples are perfectly homogeneous and consist of a regular stacking of  $\text{CdI}_2$ -type  $[\text{CoO}_2]_{\infty}$  layers stacked with triple rocksalt type layers  $[\text{Pb}_{0.7}\text{A}_{0.4}\text{Sr}_{1.9}\text{O}_3]$  ( $\text{A} = \text{Hg, Co}$ ), similarly to the misfit structure of  $\text{Ca}_3\text{Co}_4\text{O}_9$ . The intermediate rock salt layer contains lead, strontium mercury, and cobalt cations distributed at random, like in the “1201” and “1212” structures of cuprates and cobaltites. The investigation of the transport properties at 300 K shows very large thermopower values,  $S^{300\text{K}} \approx 105$  and  $115 \mu\text{V K}^{-1}$  for the Pb and (Pb/Hg)-based cobaltites, respectively, small resistivity values,  $\rho^{300\text{K}} \approx 2 \times 10^{-2} \Omega \text{ cm}$ , and the thermal conductivity measurements yield  $\kappa \approx 2 \times \text{W K}^{-1} \text{ m}^{-1}$ . The figure of merit ( $Z$ ) of these oxides is close to that of  $\text{NaCo}_2\text{O}_4$ .

### Introduction

Layered metal transition oxides exhibit very different remarkable physical properties as shown by the well-known high  $T_c$  superconductivity of copper based oxides,<sup>1</sup> the colossal magnetoresistance in layered manganese oxides,<sup>2</sup> and the room-temperature metal–insulator transition in thallium-based cobaltites.<sup>3</sup> Some years ago, a large thermopower value had been found in the metallic  $\text{NaCo}_2\text{O}_4$  cobaltite.<sup>4</sup> In this oxide, the  $\text{Co}^{3+}$  and  $\text{Co}^{4+}$  species sit in a  $\text{CdI}_2$ -type layer. The edge-shared  $\text{CoO}_6$  octahedra can be viewed as a triangular lattice of cobalt in which the low-spin (LS) state configuration of cobalt cations is stabilized.<sup>5</sup> According to Singh,<sup>6</sup> the resulting splitting of the  $\text{Co t}_{2g}$  orbitals should be responsible for the large room-temperature thermopower of this compound, with a narrow  $\text{a}_{1g}$  band giving a large density of states at the Fermi level. Recently, another class of cobaltite, called “misfit”, was discovered in which the cobalt cations sit in a similar  $\text{CdI}_2$  type layer.<sup>7</sup> In this oxide,  $\text{Tl}_{0.4}[\text{Sr}_{0.9}\text{O}]\text{CoO}_2$ , the

octahedral  $[\text{CoO}_2]_{\infty}$  layers are interleaved with rock-salt type layers, forming two bidimensional sublattices with the same symmetry but one different crystallographic “b” parameter and, consequently, incommensurate with respect to each other. Since then, several other misfit cobaltites were isolated, which were characterized by identical  $[\text{CoO}_2]_{\infty}$  layers but by thicker rock-salt type layers as illustrated by the bismuth misfit  $[\text{Bi}_{1.74}\text{Sr}_2\text{O}_4]^{RS}[\text{CoO}_2]_{1.82}$  which involves four rock-salt layers<sup>8,9</sup> and the calcium cobaltite  $[\text{CaCo}_2\text{O}_3]^{RS}[\text{CoO}_2]_{1.62}$ , called also  $\text{Ca}_3\text{Co}_4\text{O}_9$  which involves triple rock-salt layers.<sup>10–11</sup> Thus, the general formula of those misfit cobaltites can be expressed as  $[\text{AO}]_n^{RS}[\text{CoO}_2]_{\delta}$  with  $\text{A} = \text{Tl, Sr, Ca, Co, and Bi}$ , where  $n$  is the number of AO layers in the rock-salt block and  $\delta$  is the ratio between the two different cell parameters ( $\delta = b_1/b_2$ ), the subscripts 1 and 2 referring to rock-salt and  $\text{CdI}_2$  sublattices, respectively. All of the rock-salt type layers of these misfit cobaltites show striking structural similarities with that of the superconducting HTC cuprates.<sup>1</sup> In particular, a very similar stacking sequence layers of  $\text{BiO–SrO–SrO–BiO}$  is also found in the  $\text{Bi}_2\text{Sr}_2\text{Ca}_{m-1}\text{Cu}_m\text{O}_{2m+4}$  “2212-type” superconductors.<sup>1</sup> By using this simple analogy between separating rock-salt type layers of misfit cobaltites and HTCs, it naturally appeared that lead and mercury should be potential candidate to prepare new misfit cobaltites, because these cations have allowed the

\* To whom correspondence should be addressed. E-mail: Antoine.maignan@ismra.fr. Phone: 33 2 31 45 26 34. Fax: 33 2 31 95 16 00.

(1) Raveau, B.; Michel, C.; Hervieu, M.; Groult, D. *Crystal Chemistry of HTS Oxides*; Springer Series in Material Science: Berlin, 1991; Vol. 15, p 207.

(2) Moritomo, Y.; Asamitsu, A.; Kuwahara, H.; Tokura, Y. *Nature* **1996**, *380*, 141.

(3) Coutanceau, M.; Doumerc, J. P.; Grenier, J. C.; Maestro, P.; Pouchard, M.; Seguelong, T. *C. R. Acad. Sci. Paris, série IIb* **1995**, *320*, 675.

(4) Terasaki, I.; Sasago, Y.; Uchinokura, K. *Phys. Rev. B* **1997**, *56*, R12685.

(5) Mizokawa, T.; Tjeng, L. H.; Steeneken, L. H.; Schultz, K.; Sawatzky, G. A.; Brooks, N. B.; Tsukada, I.; Yamamoto, T.; Uchinokura, K. *Phys. Rev. B* **2001**, *64*, 115104.

(6) Singh, D. J. *Phys. Rev. B* **2000**, *61*, 13397.

(7) Boullay, Ph.; Domenges, B.; Hervieu, M.; Groult, D.; Raveau, B. *Chem. Mater.* **1996**, *8*, 1482.

(8) Hervieu, M.; Boullay, Ph.; Michel, C.; Maignan, A.; Raveau, B. *J. Solid State Chem.* **1999**, *142*, 305.

(9) Leligny, H.; Grebille, D.; Perez, O.; Masset, A. C.; Hervieu, M.; Michel, C.; Raveau, B. *C. R. Acad. Sci., Paris, IIc* **1999**, *409*.

(10) Masset, A. C.; Michel, C.; Maignan, A.; Hervieu, M.; Toulemonde, O.; Studer, F.; Raveau, B.; Hejtmánek, J. *Phys. Rev. B* **2000**, *62*, 166. Lambert, S.; Leligny, H.; Grebille, D. *J. Solid State Chem.* **2001**, *160*, 322.

(11) Miyazaki, Y.; Kudo, K.; Akoshima, M.; Ono, Y.; Koike, Y.; Kajtani, T. *Jpn. J. Appl. Phys.* **2000**, *39*, L531.

discovery of numerous high  $T_c$  superconductors such as the cuprates  $\text{HgBa}_2\text{Ca}_{m-1}\text{Cu}_m\text{O}_{2m+2+\delta}$ <sup>12</sup> and  $\text{Pb}_{0.5}\text{Sr}_{2.5-}\text{Ca}_{0.5}\text{Cu}_2\text{O}_{7-\delta}$ .<sup>13</sup> In the present paper, we report on the synthesis, crystal structure, and magnetic and transport properties of two new misfit cobaltites,  $[\text{Pb}_{0.7}\text{Sr}_{1.9}\text{Co}_{0.4}\text{O}_3]\text{[CoO}_2\text{]}_{1.8}$  and  $[\text{Pb}_{0.7}\text{Hg}_{0.2}\text{Sr}_{1.9}\text{Co}_{0.2}\text{O}_3]\text{[CoO}_2\text{]}_{1.8}$ .

## Experimental Section

The polycrystalline samples have been prepared by direct synthesis in contrast to the two steps used in the case of the Tl-based misfit cobaltites.<sup>7</sup> Stoichiometric amounts of oxides and peroxides,  $\text{PbO}_2$ ,  $\text{HgO}$ ,  $\text{SrO}_2$ , and  $\text{Co}_3\text{O}_4$ , were mixed and pressed in the form of bars. The latter were sealed under vacuum in silica tubes with approximately 0.8 g of sample for a volume of 3 cm<sup>3</sup> in the tube. The samples were heated to 900 °C at a heating rate of 150 °C h<sup>-1</sup>, maintained at this temperature for 12 h, and cooled to room temperature at the same cooling rate. Black ceramic bars were obtained.

The electron diffraction (ED) studies were carried out using a JEOL 200CX microscope fitted with an ecentric goniometer (±60°), whereas the high-resolution electron microscopy (HREM) images were recorded with a TOPCON 02B operating at 200kV and having a point resolution of 1.8 Å (Cs = 0.4 mm). Both microscopes are equipped with KEVEX EDS analyzers. The interpretation of experimental images was performed from HREM image simulations calculated with the Mac-Tempas multislice software. The actual cation ratio was determined from energy dispersive spectroscopy (EDS) analyses carried out on numerous crystallites.

X-ray diffraction data were collected at room temperature using of a Philips vertical diffractometer working with the Cu K $\alpha$  radiation and equipped with a secondary graphite monochromator. Lattice constants were calculated by the Rietveld method using the computer program Fullprof in the pattern matching mode, introducing two monoclinic cells (space group  $C2/m$ ) differing only by the  $b$  parameter. The same program was used for structural calculations.

The magnetic properties were studied using a SQUID magnetometer (ac and dc; 0–5 T; 1.8–400 K). Resistance data as a function of temperature (1.8–400 K) or magnetic field (0–7 T) were collected with a Quantum Design physical properties measurement system (PPMS) by the four-probe technique. Current and voltage indium contacts were ultrasonically deposited on the sintered bar (typically 2 × 2 × 10 mm). A steady-state method was used to measure the Seebeck effect and the thermal conductivity in the PPMS with high-temperature limit fixed at 320 K by the calibration range of the temperature sensors.

## Results and Discussion

Starting from nominal compositions similar to those used for the thallium misfit cobaltites,<sup>14</sup> but replacing Tl by Pb or  $\text{Pb}_{0.5}\text{Hg}_{0.5}$ , a first set of samples was investigated. For the nominal compositions  $\text{Pb}_{0.6-}\text{SrCoO}_{4.58}$  and  $\text{Pb}_{0.3}\text{Hg}_{0.3}\text{SrCoO}_{4.28}$ , two new misfit cobaltites isostructural to the pure calcium cobaltite  $[\text{Ca}_2\text{CoO}_3]\text{[CoO}_2\text{]}_{1.62}$ <sup>10,11</sup> were obtained. The EDS analyses showed that the samples were very homogeneous leading to the cationic compositions “ $\text{Pb}_{0.36}\text{SrCo}_{1.13}$ ” and “ $\text{Hg}_{0.11}\text{Pb}_{0.36}\text{SrCo}_{1.05}$ ”, respectively. A second series of synthesis was then carried out, using these cationic compositions, i.e., starting from the nominal composi-

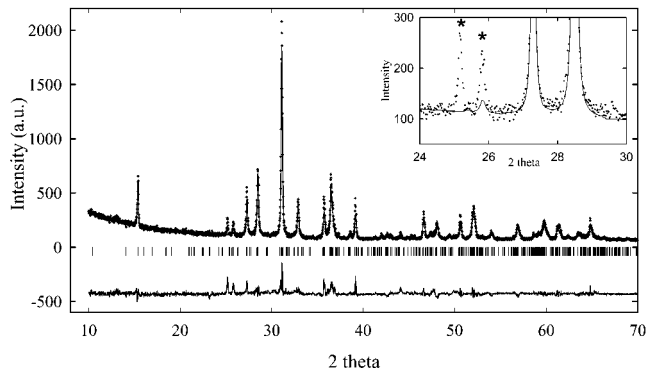


**Figure 1.** Experimental (crosses), calculated, and difference (solid lines) X-ray diffraction pattern of  $(\text{Pb}_{0.7}\text{Hg}_{0.2}\text{Sr}_{1.9}\text{Co}_{0.2}\text{O}_3)\text{[CoO}_2\text{]}_{1.8}$ . The vertical bars are the Bragg angle positions for the two 3D space group  $C2/m$  (upper  $S_1$  and lower  $S_2$ ). Inset is a magnification of a part of the patterns showing the two main peaks of  $\text{SrCO}_3$  (stars).

tions  $\text{Pb}_{0.36}\text{SrCo}_{1.13}\text{O}_{4.28}$  and  $\text{Hg}_{0.11}\text{Pb}_{0.36}\text{SrCo}_{1.05}\text{O}_{4.28}$ . For those nominal compositions, the best results were obtained, but the presence of  $\text{SrCO}_3$  as a secondary phase could not be avoided as shown from the X-ray diffraction pattern of the “PbHg” sample (Figure 1). The cationic compositions of these samples, deduced from the EDS analyses, are very close to the nominal ones, i.e., “ $\text{Pb}_{0.33}\text{SrCo}_{1.07}$ ” and “ $\text{Hg}_{0.11}\text{Pb}_{0.35}\text{SrCo}_{1.05}$ ”, respectively. The presence of several redox couples, such as  $\text{Pb}^{2+}/\text{Pb}^{4+}$ ,  $\text{Co}^{3+}/\text{Co}^{4+}$ , and  $\text{Co}^{2+}/\text{Co}^{3+}$ , has not allowed us to determine by iodometric titration the oxygen content in these cobaltites. Attempts to improve the purity by varying slightly the Sr and Co contents around those compositions were unsuccessful.

**Electron Diffraction Investigations.** The electron diffraction (ED) patterns (Figure 2) of these new phases both evidence a great similarity with the misfit cobaltites  $[\text{Tl}_{0.41}\text{SrO}_{1.12}]\text{[CoO}_2\text{]}$  and  $[\text{Ca}_2\text{CoO}_3]\text{[CoO}_2\text{]}_{1.62}$  previously studied.<sup>7,10</sup> The ED patterns of these mica-like microcrystals show indeed the coexistence in the same matrix of two monoclinic sublattices, having the same ( $a, c$ ) crystallographic plane. These two independent subsystems of these composite crystals can easily be observed along the [001] direction (Figure 2c). From these preliminary observations, the intense reflections can be indexed in two monoclinic subsystems, denoted  $S_1$  and  $S_2$ , which differ essentially by the value of  $b$  parameters. Note that no significant deviation of the  $b_1/b_2$  ratio has been detected between these oxides. The main reflections of each subsystem exhibit the same condition of reflections  $hkl: h + l = 2n$  related to C-type sublattices with cell parameters defined as follows:

$$S_1 \{a_1 \approx 5 \text{ \AA}, b_1 \approx 5 \text{ \AA}, c_1 \approx 11.5 \text{ \AA}, \text{ and } \beta_1 \approx 98^\circ\}$$

$$S_2 \{a_2 \approx 5 \text{ \AA}, b_2 \approx 2.8 \text{ \AA}, c_2 \approx 11.5 \text{ \AA}, \text{ and } \beta_2 \approx 98^\circ\}$$

$$\text{With } \delta = b_1/b_2 \approx 1.79 \approx 9/5$$

All of the incommensurate extra spots of the ED patterns (white arrows Figure 2a) using a 4D formalism ( $\mathbf{S} = h\mathbf{a}_1 + k\mathbf{b}_1 + l\mathbf{c}_1 + m\mathbf{q}_1$  with  $\mathbf{q}_1 = \delta\mathbf{b}_1$  and  $\delta = b_1/b_2$ ) can then be indexed. The  $\delta$  value equal to 1.79, close to that observed in the thallium and calcium based misfit cobaltites (1.80 and 1.62 respectively), confirms the great structural similarity of the present compounds with the misfit oxides.

(12) Antipov, E. V.; Loureiro, S. M.; Chaillout, C.; Capponi, J. J.; Bordet, P.; Tholence, J. L.; Putilin, S. N.; Marezio, M. *Physica C* **1993**, 215, 1.

(13) Rouillon, T.; Provost, J.; Hervieu, M.; Groult, D.; Michel, C.; Raveau, B. *Physica C* **1989**, 159, 201.

(14) Maignan, A.; Wang, L. B.; Hébert, S.; Pelloquin, D.; Raveau, B. *Chem. Mater.* **2002**, 14, 1231–1235.

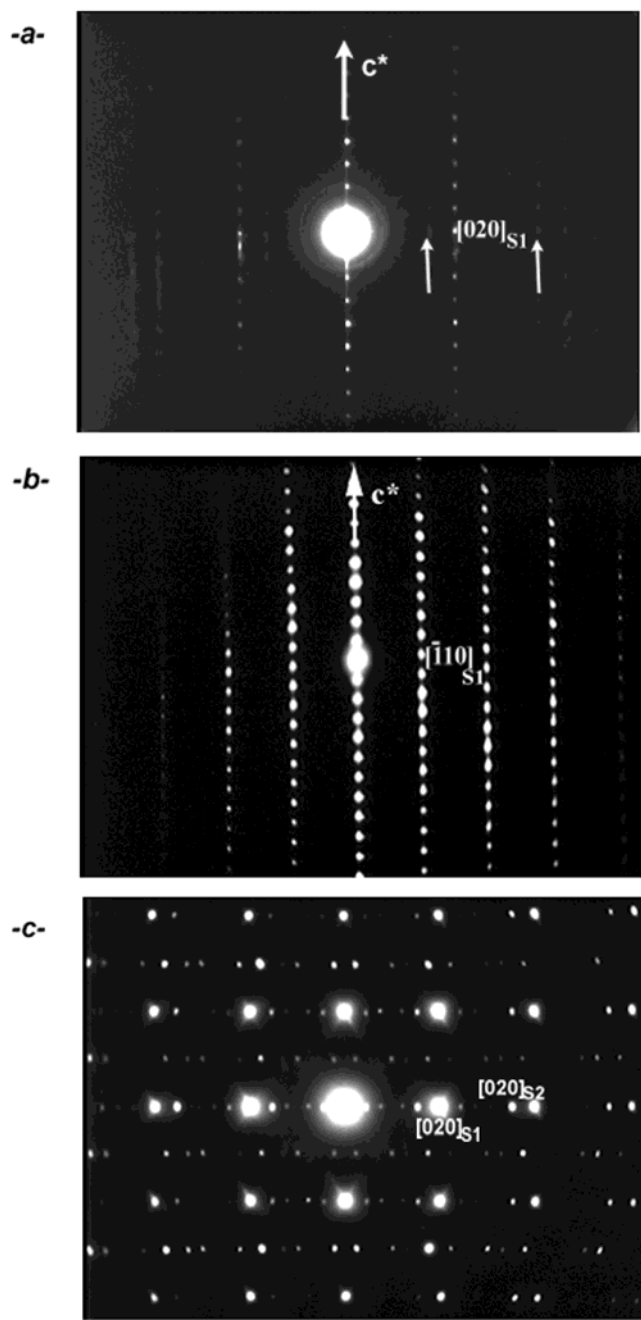


**Figure 2.** Experimental ED patterns of  $(\text{Pb}_{0.7}\text{Sr}_{1.9}\text{Co}_{0.4}\text{O}_3^-)(\text{CoO}_2)_{1.8}$  recorded along (a) [100], (b)  $[110]_{s1}$ , and (c) [001] directions.

**HREM Study: Evidence for Misfit Structures.** To identify the stacking of the different rock-salt and  $\text{CdI}_2$ -type layers along  $\bar{c}$ , a high-resolution electron microscopy investigation was first carried out along [100]. The image contrasts were interpreted by comparing the experimental images with those recorded and simulated for the misfit  $[\text{Ca}_2\text{CoO}_3][\text{CoO}_2]_{1.62}$  cobaltite.<sup>10</sup> During this study and whatever the studied sample, “ $\text{Pb}_{0.33}\text{SrCo}_{1.07}$ ” or “ $\text{Hg}_{0.11}\text{Pb}_{0.35}\text{SrCo}_{1.05}$ ”, no extended intergrowth defects or cation ordering phenomena were detected from the  $[hk0]$  oriented HREM images. Two [100] oriented images are shown in Figure 3: they have been recorded in zones belonging to the same crystallite with two different  $\Delta f$  defocus values. Whatever the focus value, the stacking sequence is composed of four specific layers. The image contrasts observed in Figure 3a, in

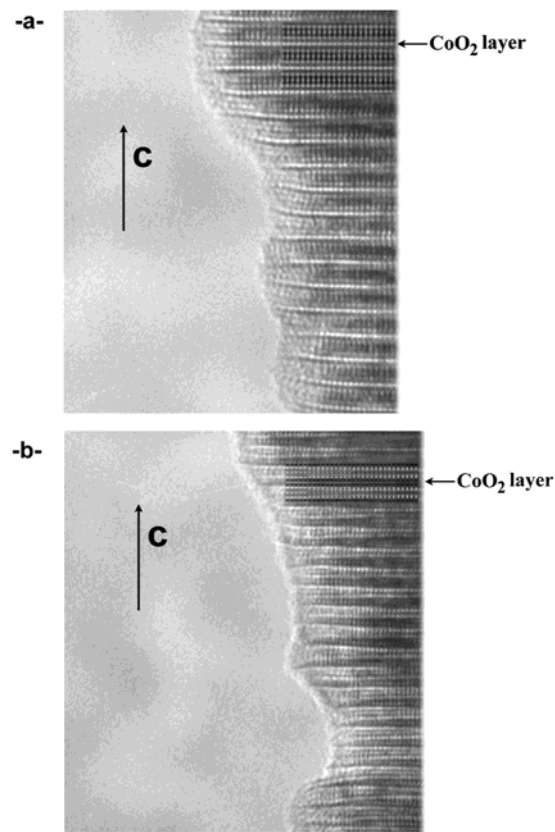


**Figure 3.** Experimental [100] oriented HREM images of Pb misfit cobaltite recorded with a defocus value close to (a) 0 and (b) 550 Å. Corresponding simulated contrasts with a thickness ranging from 26 to 56 Å are inserted.

which the high electron densities are lightened, evidence three very similar rows of gray dots interleaved by one row of bright dots along the  $c$  axis. Similar contrasts have also been reported in the  $[\text{CoCa}_2\text{O}_3][\text{CoO}_2]_{1.62}$  misfit oxide.<sup>10</sup> Taking into account the EDS results and experimental  $b_1/b_2$  ratios, cobalt species must be also introduced into the rock-salt layers leading to the complex formulations  $[\text{Pb}_{0.7}\text{Sr}_{1.9}\text{Co}_{0.4}\text{O}_3][\text{CoO}_2]_{1.8}$  and  $[\text{Pb}_{0.7}\text{Hg}_{0.2}\text{Sr}_{1.9}\text{Co}_{0.2}\text{O}_3][\text{CoO}_2]_{1.8}$ . In both cases, these sequences can be correlated to the intergrowth mechanism of three  $[\text{AO}]_{\infty}$  rock salt layers with one  $\text{CdI}_2$ -type  $[\text{CoO}_2]_{\infty}$  layer. Thus the structure of these two cobaltites  $[\text{Pb}_{0.7}\text{A}_{0.4}\text{Sr}_{1.9}\text{O}_3][\text{CoO}_2]_{1.8}$  where  $\text{A} = \text{Hg, Co}$  is derived from the  $[\text{CoCa}_2\text{O}_3][\text{CoO}_2]_{1.62}$  misfit by replacing the intermediate  $[\text{CoO}]_{\infty}$  rock salt layer by a mixed disordered  $[\text{Pb}_{0.7}\text{A}_{0.3}\text{O}]_{\infty}$  layer, whereas in the two adjacent rock salt  $[\text{CaO}]_{\infty}$  layers calcium is mainly replaced by strontium. The rock-salt nature of the  $[\text{Pb}_{0.7}\text{A}_{0.4}\text{Sr}_{1.9}\text{O}_3]_{\infty}$  layers is also confirmed by the  $[110]_{s1}$  HREM image (Figure 4) where cations are imaged as bright dots. One indeed observes triple rows of staggered bright dots spaced by 3.6 Å along  $[110]_{s1}$ , corresponding to the rock salt layers, separated along  $\bar{c}$  by single rows of brighter diffuse dots corresponding to the  $[\text{CoO}_2]_{\infty}$  layers. Note that, whatever the observation direction and experimental defocus values, the image contrasts of the triple rock-salt type layers are rather homogeneous suggesting a random distribution of lead(mercury), strontium, and cobalt species within these layers. This great ability of rock salt layers to accommodate simultaneously numerous cations, with a random distribution, is not particular to the misfit cobaltites. It has

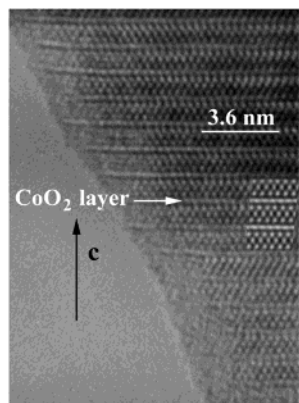


**Figure 4.** Experimental  $[110]_{s1}$  oriented HREM image of Pb misfit cobaltite and simulated contrasts calculated with a defocus value and a thickness close to 50 and 26  $\text{\AA}$ , respectively.

indeed been observed in the cuprates and cobaltites forming intergrowths between the rock salt and the perovskite structure, as shown from the 1201-type cobaltite<sup>15</sup> and the 1212-type cuprates.<sup>13</sup> This suggests, for the misfit cobaltites, a great flexibility for the incorporation of foreign cations into the structure.

**X-ray Powder Diffraction Study: Structural Approach.** The lattice parameters were refined to the following:  $a_1 = 4.9382(4)$   $\text{\AA}$ ,  $b_1 = 5.0230(5)$   $\text{\AA}$ ,  $c_1 = 11.525(1)$   $\text{\AA}$ ,  $\beta = 97.81(1)^\circ$ , and  $b_2 = 2.8018(10)$   $\text{\AA}$  for the lead compound and  $a_1 = 4.9432(4)$   $\text{\AA}$ ,  $b_1 = 5.0282(4)$   $\text{\AA}$ ,  $c_1 = 11.617(1)$   $\text{\AA}$ ,  $\beta = 97.78(1)^\circ$ , and  $b_2 = 2.8053(9)$   $\text{\AA}$  for the lead–mercury one.

It is unrealistic to establish an accurate structural determination, from X-ray powder data, for such a complex material which requires a 4D space to be considered. Nevertheless, when the incommensurate factor is close to a rational number, a 3D approach can be attempted. In both cases, the ratio  $b_1/b_2 = 1.79$ , i.e., close to  $9/5$ , allows in a first approximation a supercell to be considered with  $a = a_1$ ,  $c = c_1$ , and  $b \approx 5b_1 \approx 9b_2$ . As stated before, the assumed structural model was that of the calcium misfit cobaltite. To describe this model in the supercell, we used the space group *Cm* which is the only possible 3D space group available. Because of the great number of independent atoms (33), constraints were applied on the positional parameters of atoms in each subsystem. For example, two adjacent identical atoms along  $\bar{b}$  should have same  $x$  and  $z$  values, with  $y$  differing by  $1/5$  in the rock-salt-type part and by  $1/9$  in the CdI<sub>2</sub>-type part. Isotropic thermal factors were fixed to  $B = 0.8$  and  $1.5$   $\text{\AA}^2$  for metals and oxygens, respectively. Because the model is an approximated 3D supercell, the oxygen sites, especially their occupancy factor, cannot be accurately refined. So no oxygen vacancy was considered. Heavy cations were preferably located in the central layer of the rock-salt-type subsystem without any distinction between lead and mercury because of their similar scattering factor. SrCO<sub>3</sub> was introduced as secondary phase in the calculations.

For these conditions, the refined  $b$  lattice constant of the supercell for the mixed lead/mercury cobaltite was  $b = 25.134(1)$   $\text{\AA}$ . Refinement results are listed in Table

**Table 1. Structural Parameters for a 3D Supercell, Space Group *Cm* with  $a = 4.9432(4)$   $\text{\AA}$ ,  $b = 25.134(1)$   $\text{\AA}$ ,  $c = 11.617(1)$   $\text{\AA}$ ,  $\beta = 97.78(1)^\circ$ ,  $R_B = 0.090$ ,  $R_p = 0.119$ ,  $R_{wp} = 0.161$ , and  $\chi^2 = 2.06^a$**

atom	site	$x$	$y$	$z$	$B$ ( $\text{\AA}^2$ )	$\tau$
Rock-Salt-Type Part						
Pb(1)	$2a$	0.0	0.0	0.5	0.8	0.83(3) <sup>b</sup>
Pb(2) <sub>i</sub>	$4b$	0.0	1/5	0.5	0.8	0.83(3) <sup>b</sup>
O(1)	$2a$	0.5	0.0	0.5	1.5	1.0
O(2) <sub>i</sub>	$4b$	0.5	1/5	0.5	1.5	1.0
Sr(1)	$2a$	0.430(1)	0.0	0.2675(4)	0.8	1.13(2) <sup>c</sup>
Sr(2)	$2a$	-0.430(1)	0.0	-0.2675(4)	0.8	1.13(2) <sup>c</sup>
Sr(3) <sub>i</sub>	$4b$	0.430(1)	1/5	0.2675(4)	0.8	1.13(2) <sup>c</sup>
Sr(4) <sub>i</sub>	$4b$	-0.430(1)	1/5	-0.2675(4)	0.8	1.13(2) <sup>c</sup>
O(3)	$2a$	0.951(7)	0.0	0.320(3)	1.5	1.0
O(4)	$2a$	-0.951(7)	0.0	-0.320(3)	1.5	1.0
O(5) <sub>i</sub>	$4b$	0.951(7)	1/5	0.320(3)	1.5	1.0
O(6) <sub>i</sub>	$4b$	-0.951(7)	1/5	-0.320(3)	1.5	1.0
CdI <sub>2</sub> -Type Part						
Co(1)	$2a$	0.75	0.0	0.0	0.8	1.0
Co(2) <sub>j</sub>	$4b$	0.75	1/9	0.0	0.8	1.0
O(7)	$2a$	0.380(6)	0.0	-0.085(2)	1.5	1.0
O(8)	$2a$	0.120(6)	0.0	0.085(2)	1.5	1.0
O(9) <sub>j</sub>	$4b$	0.380(6)	1/9	-0.085(2)	1.5	1.0
O(10) <sub>j</sub>	$4b$	0.120(6)	1/9	0.085(2)	1.5	1.0

<sup>a</sup> Constraints: For  $i = 1$  to 2,  $y_{i+1} = y_i + 1/5$  and for  $j = 1$  to 4,  $y_{j+1} = y_j + 1/9$ .  $X_{\text{Sr}(1)} = X_{\text{Sr}(2)} = -X_{\text{Sr}(3)} = Z_{\text{Sr}(1)} = Z_{\text{Sr}(3)} = -Z_{\text{Sr}(2)} = -Z_{\text{Sr}(4)}$ .  $X_{\text{O}(3)} = X_{\text{O}(5)} = -X_{\text{O}(4)} = -X_{\text{O}(6)}$ ,  $Z_{\text{O}(3)} = Z_{\text{O}(5)} = -Z_{\text{O}(4)} = -Z_{\text{O}(6)}$ .  $X_{\text{O}(7)} = X_{\text{O}(9)} = 1/2 - X_{\text{O}(4)} = 1/2 - X_{\text{O}(6)}$ ,  $Z_{\text{O}(3)} = Z_{\text{O}(5)} = -Z_{\text{O}(4)} = -Z_{\text{O}(6)}$ . <sup>b</sup> Parameters fixed at the same value.

1. Because of the considered structural simplifications, the value of the different agreement factors ( $R_p = 0.119$ ,  $R_{wp} = 0.161$ ,  $R_B = 0.090$ , and  $\chi^2 = 2.06$ ) and the X-ray powder difference pattern (bottom of Figure 1) attest of the validity of the model. The structure is drawn in Figure 5. It should be noted that the fit quality is greatly improved by refining the site occupancy of Pb(Hg) and Sr. The results (Table 1) show that the central AO plane of the rock salt slice is not completely occupied by the posttransition metals, whereas some Pb and (or) Hg atoms are distributed over the Sr sites (site occupancy greater than 1). The composition of the theoretical SrO layers which can be deduced from the strontium site occupancy is then  $\text{Sr}_{0.9}(\text{Pb}, \text{Hg})_{0.1}\text{O}$ . Under these conditions to agree with EDS analysis ( $(\text{Hg} + \text{Pb}):\text{Sr}:\text{Co} = 0.46:1:1.05$ ), it appears that the intermediate rock salt layer should play the role of reservoir for accommodation of various cations, being simultaneously occupied by “Hg and Pb” (~70%), Co (~20%), and Sr (~10%). These occupancy factors cannot be considered as accurate, but they show a partial disorder inside the rock salt subsystem which is confirmed by the study of the misfit mercury free cobaltite ( $\tau = 0.58$  for Pb sites and  $\tau = 1.06$  for Sr sites). As stated above, rock salt layers with cationic sites occupied simultaneously by a post transition metal and a transition metal or an alkaline earth have already been observed in other systems.

From these refined atomic positions, especially the nature of three mixed [AO] rock-salt-type layers deduced from occupation site values (cf. Table 1), simulated HREM images have been carried out along the main studied directions, namely,  $[100]$  and  $[110]_{s1}$ . These calculations performed with a crystal thickness ranging from 26 to 56  $\text{\AA}$  are inserted in the experimental HREM images previously described (Figures 3 and 4). These calculated contrasts fit perfectly the experimental ones, especially along the  $[110]_{s1}$  direction for which the

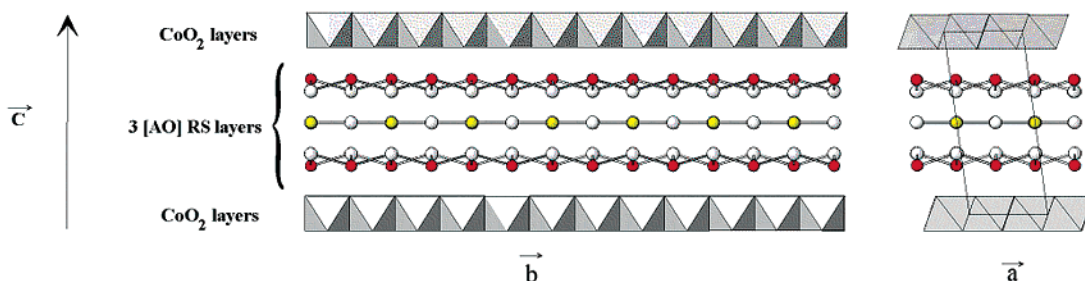


**Figure 5.** Drawing of the structure of the lead and lead–mercury misfit cobaltites viewed along a (left part)  $\bar{a}$  and  $\bar{b}$  (right part) axis showing the three rock-salt-type AO layers sandwiched by two  $\text{CoO}_2$  layers. Pb and Hg are mainly located in the intermediate (central) AO layer of the rock salt part.

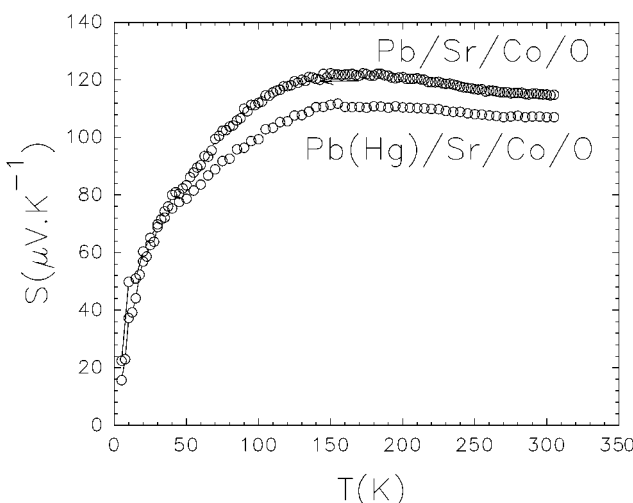


**Figure 6.**  $T$  dependence of the thermopower (Seebeck  $S$ ) for both  $\text{Pb/Sr/Co/O}$  and  $(\text{Hg/Pb})/\text{Sr/Co/O}$  misfit cobaltites.

typical rocksalt layers contrasts are easily identified, and valid the structural model.

**Magnetic and Transport Properties.** One interesting property of the Tl-, Bi/Pb-, and Ca-based misfit cobaltites lies in their large thermopower ( $S$ ) at room temperature, always in the range of  $90\text{--}130\text{ }\mu\text{V K}^{-1}$ .<sup>4,10\text{--}11,16\text{--}18</sup> A similar value was also reported for  $\text{NaCo}_2\text{O}_4$ ,  $S^{300\text{K}} = 100\text{ }\mu\text{V K}^{-1}$ .<sup>4</sup> From all of these thermopower results, it is tempting to associate the large  $S$  value with the peculiar  $\text{CoO}_2$  layer common to all of these oxides. The thermopower values obtained here for the  $[\text{Pb}_{0.7}\text{A}_{0.4}\text{Sr}_{1.9}\text{O}_3][\text{CoO}_2]_{1.8}$  misfit cobaltite reinforce this hypothesis. As shown in Figure 6, at room temperature the values for both  $\text{Pb/Sr/Co/O}$  and  $(\text{Hg/Pb})/\text{Sr/Co/O}$  misfits are found to be close to  $110\text{ }\mu\text{V K}^{-1}$ . Interestingly, this value is also close to that reported for  $\text{Ti/Sr/Co/O}$ ,  $S^{300\text{K}} = 90\text{ }\mu\text{V K}^{-1}$ .<sup>18</sup> However, the transport properties of the latter misfit are unique among these cobalt oxides because it is the only one which remains metallic down to 2 K. In this respect, it is not very surprising to observe an upturn in the resistivity at low  $T$  for the present compounds as for all of the other misfits except the Tl-based one (Figure 7). The  $\rho(T)$  curves exhibit thus a  $\rho$  minimum at about  $T_{\min} = 100$  and  $70$  K for the pure Pb and mixed Hg/Pb cobaltites, with the localization effect of the former

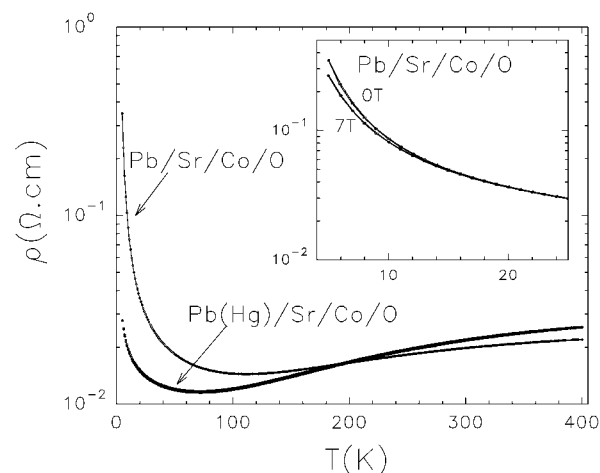


**Figure 7.**  $T$  dependence of the resistivity  $\rho$  for the  $\text{Pb/Sr/Co/O}$  and  $(\text{Hg/Pb})/\text{Sr/Co/O}$  misfit cobaltites. Inset: low  $T$  enlargement.

below  $T_{\min}$  being much more pronounced,  $\rho_{T_{\min}}/\rho_{2\text{K}} = 17$  against 2.3 for the latter. Despite these very different low  $T$  resistivity values, the values at 300 K are very close for the two cobaltites  $\rho^{300\text{K}} \sim 2 \times 10^{-2} \Omega \text{ cm}$ , which is very similar to that of  $\text{Ti/Sr/Co/O}$ ,  $\rho^{300\text{K}} = 2.4 \times 10^{-2} \Omega \text{ cm}$ .<sup>18</sup> The transport properties of these new Pb and (Hg/Pb) misfit cobaltites are very close to that of  $\text{Ca}_3\text{Co}_4\text{O}_9$  which exhibits similar  $S(T)$  and  $\rho(T)$  characteristics.<sup>10\text{--}11</sup> This is also illustrated by the negative magnetoresistance (MR) of Pb- and (Hg/Pb)-based cobaltites which was also found in  $\text{Ca}_3\text{Co}_4\text{O}_9$ . This feature is shown in the low  $T$  enlargement of the  $\rho(T)$  curves collected by cooling in the absence (0 T) and in the presence of a 7 T magnetic field (Pb/Sr/Co/O curves in the inset of Figure 7). The two curves start to deviate below 18 K, with the  $\rho_{7\text{T}}(T)$  curve starting to run below the  $\rho_{0\text{T}}(T)$  one below that temperature. As it has been shown for several cobaltites, the MR magnitude is larger as the localized character becomes more pronounced; for instance, in the  $\text{La}_{1-x}\text{Sr}_x\text{MnO}_3$  perovskite, the MR is the smallest for the most metallic compositions.<sup>19</sup> This assertion is also verified in our case at 2 K and in 7 T, where the MR, defined as  $\text{MR} = 100(\rho(\text{H}) - \rho(\text{O})/\rho(\text{O}))$ , reaches only  $-15\%$  in the Hg/Pb-based misfit against  $-80\%$  in the Pb based one (Figure 8). Such a very high value is of the same order as that reported for the weakly ferromagnetic (Bi/Pb)-misfit cobaltite,  $-55\%$  in 8 T at 2 K.<sup>20</sup> In contrast, it should also be pointed out that the MR of the paramagnetic  $\text{Ti/Sr/Co/O}$  misfit is

(16) Itoh, T.; Kawata, T.; Kitajima, T.; Terasaki, I. *Int. Conf. Thermoelectr. Proc.* **1998**, 17, 595.

(17) Itoh, T.; Terasaki, I. *Jpn. J. Appl. Phys.* **2000**, 39, 6658.

(18) Hébert, S.; Lambert, S.; Pelloquin, D.; Maignan, A. *Phys Rev B* **2000**, 64, 172001.

(19) Mahendiran, R.; Raychaudhuri, A. K. *Phys. Rev. B* **1996**, 54, 16044.

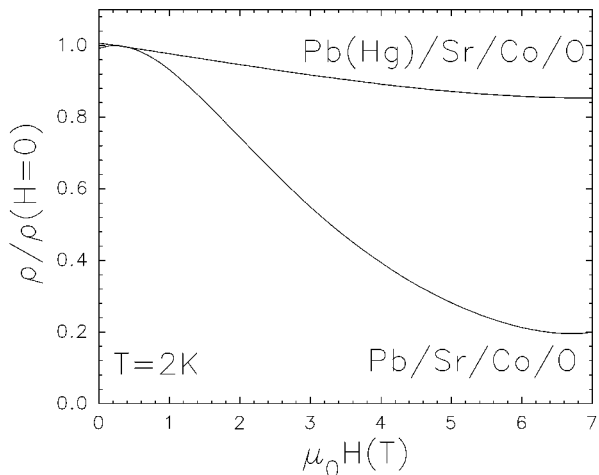


**Figure 8.** Magnetic field ( $H$ ) dependence of  $\rho/\rho(H=0)$  for both studied cobaltites ( $T=2\text{ K}$ ).

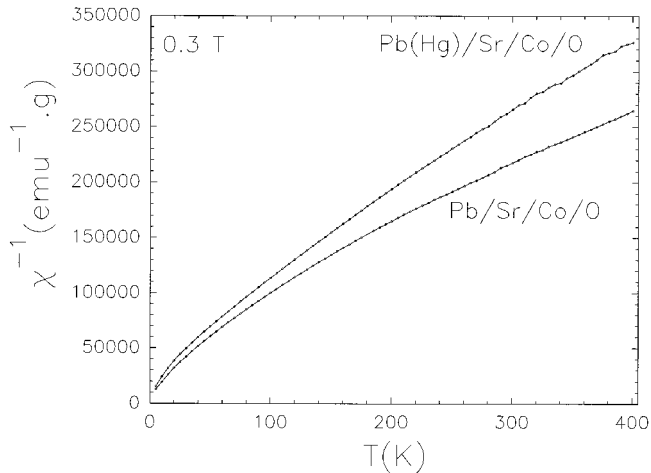


**Figure 9.**  $\chi^{-1}(T)$  curves for both misfit cobaltites.

positive and small,  $\text{MR}_{2\text{K},7\text{T}} = +5\%$ .<sup>18</sup> The differences in the low-temperature MR could originate in the spin polarized transport. Weak  $\mu_{\text{eff}}$  values, slightly larger for the Pb-based misfit, are obtained for these phases from the high  $T$  part ( $200\text{ K} \leq T \leq 400\text{ K}$ ) of the  $\chi^{-1}(T)$  curve. They can be attributed to the low spin state of both  $\text{Co}^{3+}$  and  $\text{Co}^{4+}$  which lie in the  $\text{CoO}_2$  layer.<sup>5</sup> However, the  $\chi^{-1}(T)$  curves (Figure 9) of these samples do not show any transition associated with long-range magnetic ordering.

The similarity of the transport and magnetoresistance properties of these new “Pb” and “Pb–Hg” misfit cobaltites with the misfit Ca and the “BiPb” cobaltites<sup>20</sup> suggests strongly that the thermoelectric power properties originate from the  $\text{CoO}_2$  layers with  $\text{Co}^{3+}/\text{Co}^{4+}$  in low-spin states rather than in the separating layers which can be of very different chemical natures. The difference with the Tl/Sr/Co/O misfit, which exhibits a positive MR and paramagnetic state, could be explained by the absence of spin-scattering in the Tl-based misfit. Changes in the mobile carrier concentration and changes

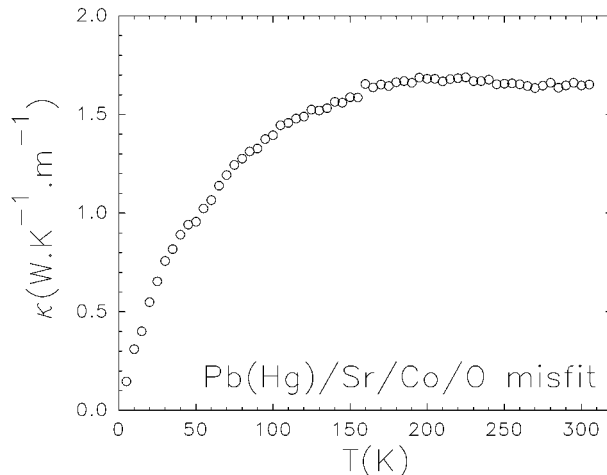


**Figure 10.**  $T$ -dependent thermal conductivity for the  $\text{Pb}(\text{Hg})/\text{Sr}/\text{Co}/\text{O}$  misfit cobaltite.

in the effective mass of charge carriers induced by the different cations in the rock-salt-type layers will have to be checked in the future by Hall effect and specific heat measurements on crystals.

The low resistivity of these misfit cobaltites as well as their high  $S$  values at room temperature suggest possible thermoelectric applications in the field of energy conversion technology. Considering the figure of merit  $Z = S^2/\rho\kappa$ , where  $S$ ,  $\rho$ , and  $\kappa$  are the thermopower, resistivity, and thermal conductivity, respectively,  $\kappa(T)$  measurements have been carried out. As shown in Figure 10 for  $[\text{Pb}_{0.7}\text{Hg}_{0.2}\text{Sr}_{1.9}\text{Co}_{0.2}\text{O}_3][\text{CoO}_2]_{1.8}$ , the  $\kappa$  value at room temperature equal to about  $2\text{ W K}^{-1}\text{ m}^{-1}$  is close to that observed for  $\text{NaCo}_2\text{O}_4$  and  $\text{Ca}_3\text{Co}_4\text{O}_9$ .<sup>10–11</sup> As a result, the figure of merit at  $300\text{ K}$ ,  $Z^{300\text{K}} \approx 3 \times 10^{-5}\text{ K}^{-1}$ , is about three times smaller than that reported for the best cobalt oxide  $\text{NaCo}_2\text{O}_4$  ( $Z^{300\text{K}} \approx 1.1 \times 10^{-4}\text{ K}^{-1}$ ). Both cobaltites exhibit  $ZT$  values at  $300\text{ K}$  much smaller than the required value  $ZT = 1$  for room-temperature applications but appear promising for high temperature utilization.

## Conclusions

This study shows the great flexibility of the rock salt layer in the misfit cobaltites, which is able to accommodate various cations such as mercury, lead, cobalt, and strontium distributed at random. In this respect, this behavior is similar to that observed for “1201” and “1212” intergrowths obtained for high  $T_c$  superconductors, and several cobaltites, whose rock salt type layers also accommodate numerous foreign cations. The TEP and resistivity measurements evidence high  $S$  values and small resistivity values at room temperature, like for other misfit cobaltites, demonstrating that the  $[\text{CoO}_2]_\infty$  layers play a prominent role in the transport properties of these materials. Further investigations should be carried out to understand the influence of the rock salt layers on the properties of this large family of misfit cobaltites which appears promising for thermoelectric applications at high temperature.

(20) Yamamoto, T.; Tsukuda, I.; Uchinokura, K.; Takagi, M.; Tsubone, T.; Ichihara, M.; Kobayashi, K. *Jpn. J. Appl. Phys.* **2000**, *39*, L747.